








Reliance on fossil fuels increases during extreme temperature events in the continental United States

Wenli Zhao ^{1,2}✉, Biqing Zhu ³, Steven J. Davis ⁴, Philippe Ciais ³, Chaopeng Hong ⁵, Zhu Liu ⁶ & Pierre Gentine ¹✉

Increasing extreme climate events driven by climate change raise the question of their impacts on the power production system, and implications for renewable versus fossil power supply. Here, using climate reanalysis data and daily electricity generation (2018–2023), we systematically quantify the impact of extreme climate events, specifically extreme cold events and extreme hot events on United States state-level carbon emissions and on the carbon intensity of electricity. We find that extreme climate events increase the carbon intensity of the energy production, increasing the reliance on fossil-based sources of energy and reducing the capacity of renewables. The states with more renewable electricity generation were also more affected by extreme temperatures. Our results reveal the extent to which the reliability and resilience of the current United States electricity system depends on fossil energy during extreme climate events, and suggest a need for adaptation measures as the country will transition to higher shares of renewable energy while extreme events will become more frequent.

¹Columbia University, New York, NY, USA. ²Max Planck Institute for Biogeochemistry, Jena, Germany. ³Laboratoire des Sciences du Climat et de l'Environnement (LSCE), Gif-sur-Yvette, France. ⁴Department of Earth System Science, University of California Irvine, Irvine, CA, USA. ⁵Tsinghua Shenzhen International Graduate School, Shenzhen, China. ⁶Tsinghua University, Beijing, China. ✉email: dr.wenli.zhao.pku@gmail.com; happystillwaterzhao@gmail.com; pg2328@columbia.edu

The intensity and frequency of winter storms, droughts, heatwaves, and other extreme events have increased in recent decades as a result of climate change^{1,2}, and numerous studies expect this trend to further intensify^{3–5}. In turn, extreme events have been shown to impact electricity systems, causing disruptive increases in power demand for heating or cooling and sometimes deadly outages^{6–10}. Large-scale outages are due to a regional imbalance between electricity generation and demand, which can occur because of failures in electricity generation or transmission infrastructure, when surging demand outstrips available generation, or both. Extreme heat greatly increases electricity demand for air conditioning and extreme cold increases electricity demand in regions where some heating systems are electric^{11–16}. High temperatures decrease the operating efficiency of thermal power plants and solar photovoltaics, droughts limit hydroelectric generation^{17–20}. Very cold temperatures and winter storms can freeze cooling and fuel pipes or wind turbines²¹.

However, the specific impacts of extreme climate events on fossil and renewable energy electricity generators remain unclear. There is widespread concern that renewable energy systems could be more susceptible to disruptions under extreme conditions, indicating their vulnerability^{22,23}. This calls for a thorough and comprehensive investigation to better understand the potential vulnerabilities of renewable energy sources during extreme climate events. If fossil energy sources prove more reliable during extremes, increasing frequency and intensity of extreme events would work against mitigation efforts. Yet many states, countries, and companies have announced plans to drastically reduce fossil energy as they target net-zero emissions^{24,25}. Among all scenarios assessed by the most recent IPCC report (AR6)¹, renewable energy sources is projected to supply an average of 63% of the world's primary energy in the year of 2070 when global CO₂ emissions reach net-zero ($n = 476$, which indicates number of the scenarios). For 1.5 and 2 °C net-zero scenarios, renewable sources represent an average of 64% of primary energy when they reach net-zero CO₂ emissions in the year of 2068.

Here, therefore, we systematically evaluate electricity generation, its carbon emission and carbon intensity (emission per unit of electricity generated) variations with daily temperatures across the U.S. (48 states + Washington D.C.) over the period of 2018–2023 to quantitatively characterize how the electricity production systems responded to extremes in recent years. Details of our analytical approach are available in the Supplementary Materials (Supplementary Methods and Supplementary Fig. 1). In summary, we use electricity generation data from the U.S. Energy Information Administration (EIA)²⁶ at state level and air temperature data from the ERA5-Land reanalysis²⁷ to assess the sensitivity of daily, state-level electricity generation, carbon emissions and carbon intensity to population-weighted surface air temperatures (calculated from pixel-level, see Supplementary Methods), and especially temperature extremes. Note that extreme events here, are based on long-term historical air temperature data extreme detection, which will only see the change in unbiased variance (Supplementary Methods).

Results

Emissions and carbon intensity increase sharply during extreme temperature events. In general, 5212 extreme hot events or days in June/July/August (JJA) (defined by single days with extreme hot population-weighted air temperature, see Supplementary Methods) and 2632 extreme cold events or days in December/January/February (DJF) (defined by single days with extreme cold population weighted air temperature) were selected based on 95% and 5% percentiles of 34 years' (1990–April 2023)

local population weighted daily air temperature (Ta) distributions for 48 U.S. states + Washington D.C. (see Supplementary Methods). More extreme hot days were detected than extreme cold days over the study period (July 2018 to April 2023), as seen in Fig. 1, Supplementary Fig. 2, Supplementary Fig. 3, Supplementary Fig. 4, Supplementary Fig. 5 and Supplementary Fig. 6. We found that, during both extreme periods (hot and cold), emissions increase sharply for most of the impacted U.S. states (Fig. 1, Fig. 2, Supplementary Fig. 2, Supplementary Fig. 3, Supplementary Fig. 4, Supplementary Fig. 5). Importantly, we also found that the increasing emissions are always accompanied by an increasing carbon intensity, clearly seen in the time series plots compared to non-extreme Ta periods (see Supplementary Methods) (Fig. 1c, d). This is consistent with previous studies²⁸.

Extreme high Ta and low Ta days together (accounting for 20.3% of the days over the summer and winter time during the study period from July 2018 to April 2023) account for 22.5% of carbon emissions for the summer + winter time during the study period (July 2018 to April 2023) for the 48 U.S. states + D.C. The ratio of carbon emissions during all hot and cold extremes to total emissions differs across different U.S. states possibly due to differences in local energy mix and grid inter-connections, available renewable resources and severity of climate extremes (Supplementary Fig. 6). Extreme cold days (15.0% of the winter time) account for 18.1% of the carbon emissions from the winter time. Extremely hot days (24.7% of the summer time) account for 25.4% of the carbon emissions of the summer time. During all extreme events, the 48 U.S. states + D.C. rely on more fossil energy to generate 13.9% of total power in the summer and winter throughout the study period, with 4.5% coming from cold days and 9.4% from hot days. For the 12 warmest states, defined as the states with the top 12 highest annual mean temperatures, all climate extremes (17.8% of the summer + winter time) account for 21.5% of total fossil fuels emissions, split between 7.5% for extreme cold events (6.9% of the summer + winter time) and 14.0% for extreme hot events (occurring 10.9%), respectively. For the 12 coldest states, defined as the states with the top 12 lowest annual mean temperatures, all climate extremes (23.9% of the summer + winter) represent 25.5% of total fossil fuels emissions, split between 8.5% for cold days (occurring 7.9% of the summer + winter) and 17.0% for hot days (occurring 16.0%), respectively.

Our analysis of each power production source shows that during climate extremes, the share of fossil fuel production is increasing, especially natural gas, while at the same time the proportion of renewables decreases, e.g., solar, wind and hydro power (Fig. 1, Supplementary Figs. 2, 3, 4, 5). Note that our analysis of 34 years' air temperature also shows that the air temperature during the summer exhibits a clear increasing tendency during the recent years (Supplementary Figs. 7, 8). This implies that extreme hot days became more frequent and more intense in recent years^{29–31}.

Extreme temperature events increase emissions and reliance on fossil fuel across U.S. states. All the detected extreme Ta events (extreme cold and hot events) for all U.S. states are summarized in Fig. 2. Specifically, for the cold events, about 48 U.S. states + D.C. show an average 23.5% increase in carbon emission across the U.S. between extreme cold days and normal days (defined as the first temperature inflection point which is higher than 10th percentiles, see Supplementary Methods). The share of fossil fuel power in these states also increased by 5.4%, correspondingly (Fig. 2). This indicates a generally 'dirtier' power generation during local cold weather extremes (Figs. 1, 2). Similarly, during extreme hot days, 46 states show an increase of carbon emission,

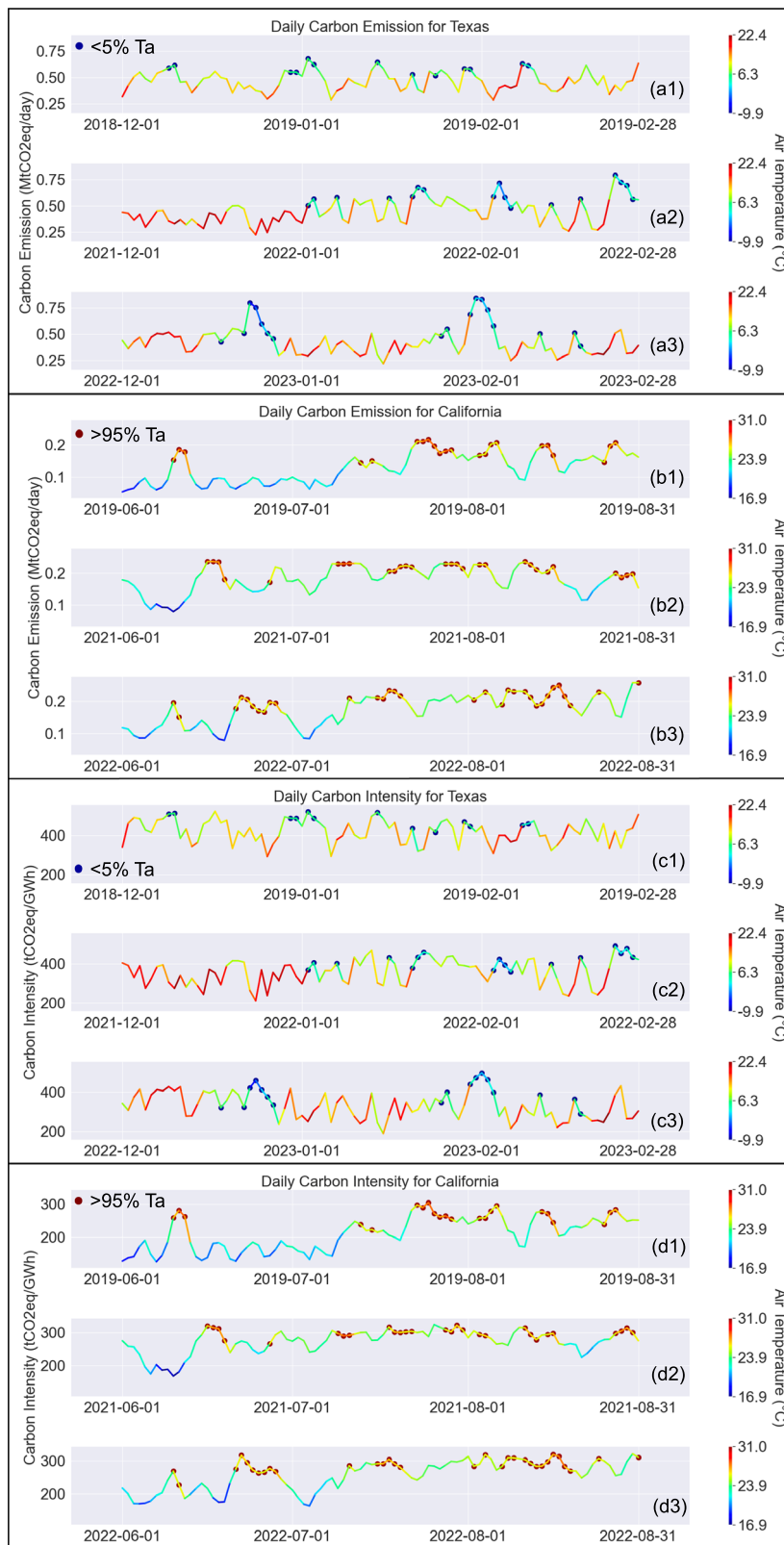
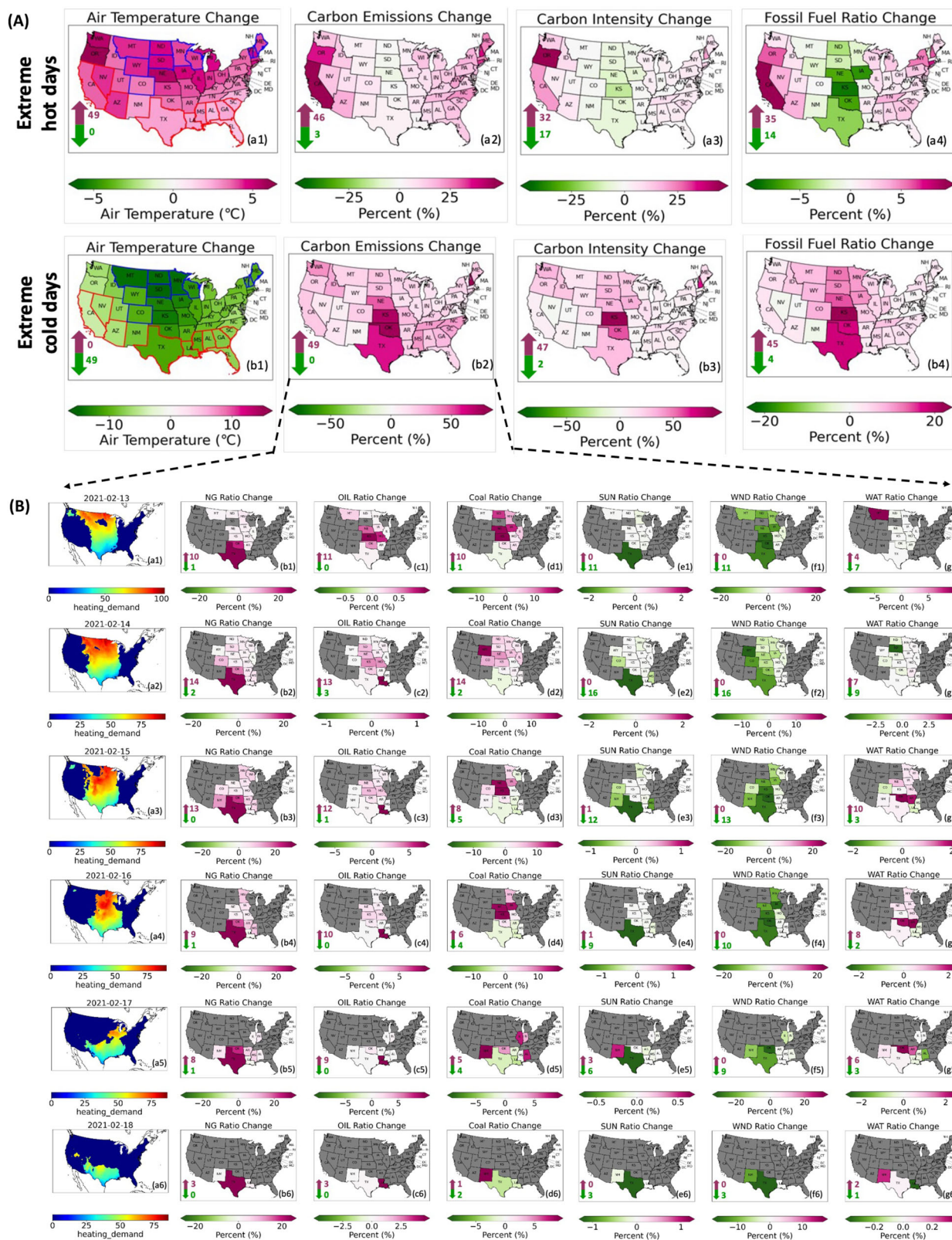


Fig. 1 Daily carbon emission and carbon intensity for selected U.S. states. **a, b** Indicate the carbon emission for selected states (Texas and California) for winter (December, January, February) and summer (June, July, August), respectively. **c, d** indicate the corresponding carbon intensity for the selected states during winter and summer, respectively. Number 1, 2, 3 indicate different years. Other examples are not shown here due to the limit of main text (see supplementals). Note the line is shading with population-weighted air temperature. The left end of the line segment represents the corresponding daily mean population weighted temperature. The dots in the lines indicate the detected extreme air temperatures, dark blue dots for T_a less than 5% percentiles local population weighted air temperature during 34 years (1990–2023), dark red dots for T_a larger than 95% local population weighted T_a during 34 years (1990–2023). Note that December 2019, January 2020, February 2020 is excluded for the following analysis due to the impact of COVID.



by 14.1% compared to normal days. In 35 of these states the share of fossil fuel is increasing by 2.6% on average during extreme hot days.

For the response to extreme hot days, we found that 14 states showing declining shares of fossil energy are mainly located in the central region of the United States. A further check shows that for those 14 states with decreasing shares of fossil power and carbon

emissions during hot days, the share of fossil fuel is declining by 3.3% while renewables increased by 3.8% (Supplementary Fig. 9). This potentially shows that there exist better conditions for renewable resources during extreme hot days. Although extreme hot days can lead to a decrease in the efficiency of photovoltaic (PV) systems^{32–35}, they also coincide with higher solar irradiance levels. As a result, the proportion of solar energy generation in the

Fig. 2 Maps of changes of air temperature, carbon emission, carbon intensity and fossil fuel ratio of power production for all hot and cold extreme temperature events. **A** Mean value for the whole study period. a indicates the extreme cold events. Ta less than 5% percentiles local population weighted air temperature during 34 years (1990-2023). b indicates extreme hot events. Ta larger than 95% percentiles local population weighted Ta during 34 years (1990-2023). Number 1 indicates average population-weighted air temperature changes for extreme events, compared to the normal days. Number 2 indicates average carbon emission percent changes for extreme events, compared to the normal days. Number 3 indicates average carbon intensity percent changes for extreme events, compared to the normal days. Number 4 indicates the average share of fossil fuel changes for extreme events, compared to the normal days. The purple upward arrows and numbers in the lower left corner of each subplot indicate the number of states with increasing values, and green downward arrows and numbers indicate the number of states with decreasing values. Cold states with a blue border in a1 and b1, with the top 12 lowest annual mean temperatures. Warm states with a red border, with the top 12 highest annual mean temperatures (see Supplementary Methods). **B** An example for a sub-energy component analysis of a 6-day consecutive extreme cold event. (a) Heating demand index (HDD) is from Doss-Gollin, et al., (2021). The unit is F degree. When the HDD is greater than 0, it indicates a heating demand. The larger this index is, the greater the heating demand is during extreme cold days. The share of (b) Natural gas, (c) Oil, (d) Coal, (e) Solar, (f) Wind, (g) Hydro change during the widely reported extreme cold days in February 2021 (Winter storm “Uri”). NG is for Natural gas, SUN is for solar energy, WND wind power, WAT hydro power.

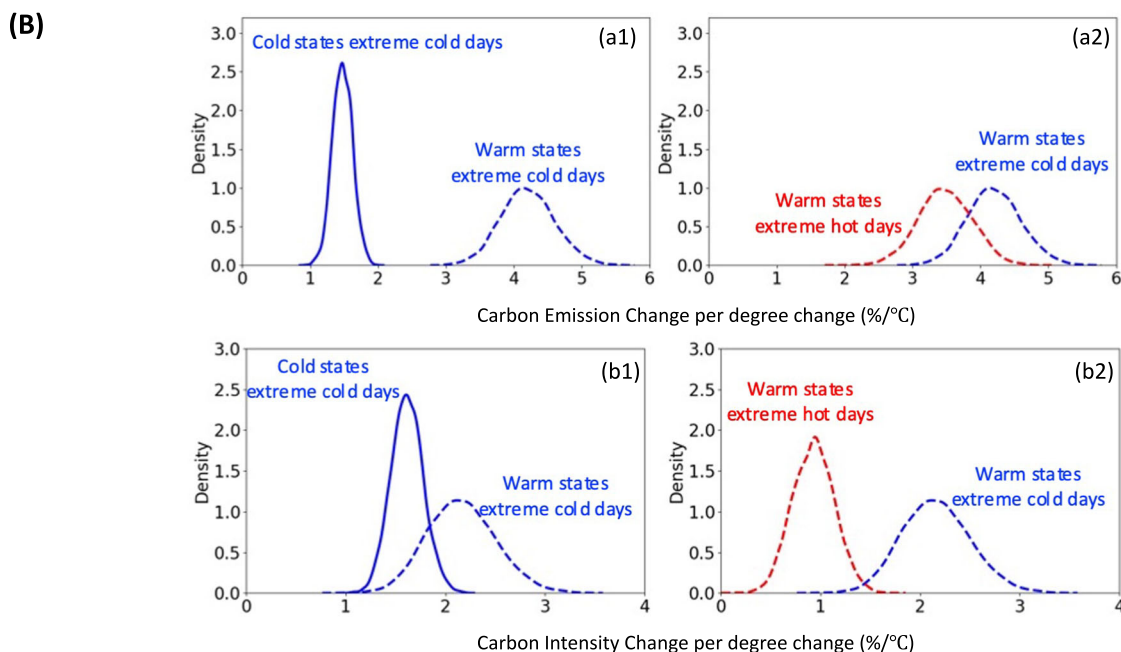
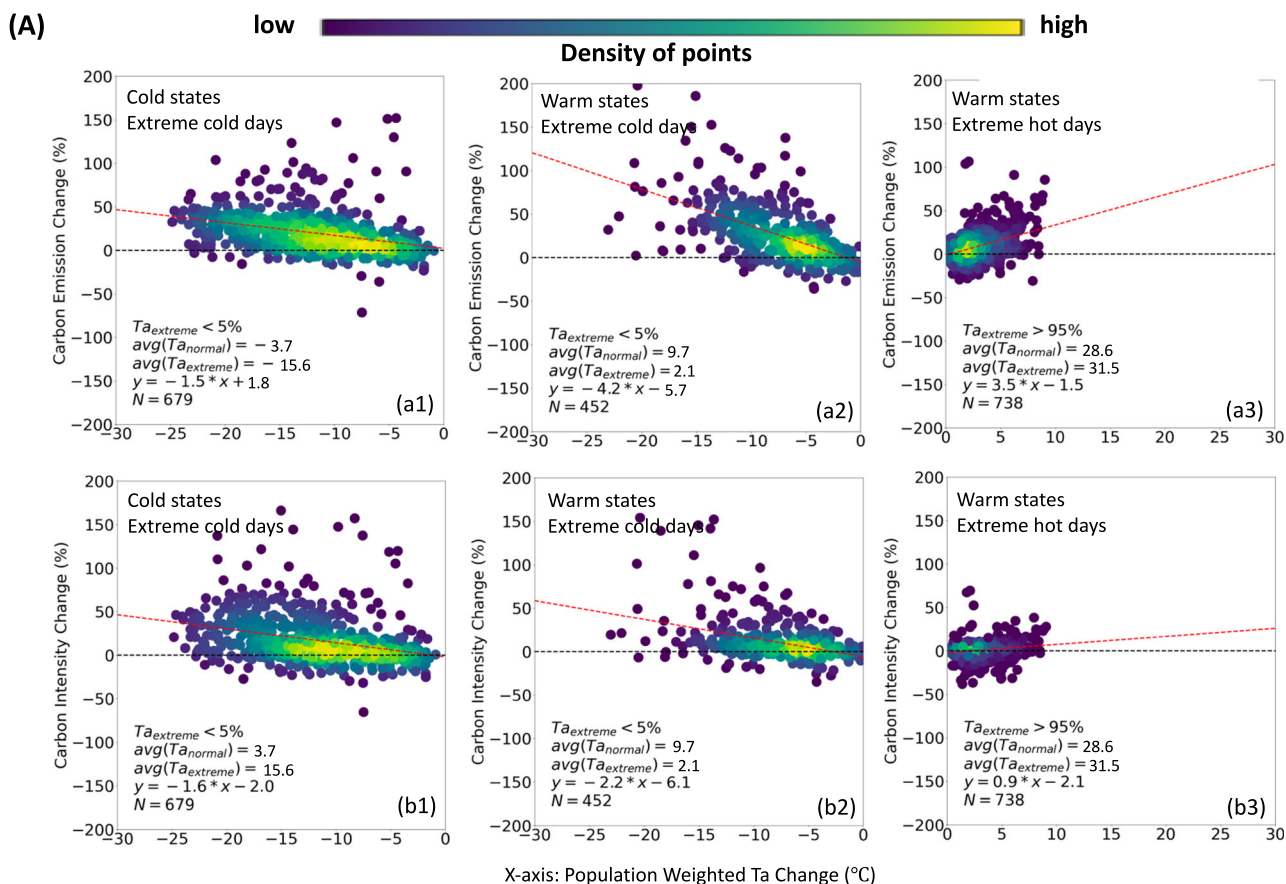
electricity mix possibly tends to increase. Specifically, our findings indicate an average increase of 0.1% in the share of solar energy during extreme hot days, which could not match entirely the increasing demand for electricity^{36,37} (Supplementary Fig. 9). However, in summer time, the 14 states in central region with high wind power generation capacity has relatively more wind power resources than the eastern and western region of the country^{38–40}. Our analysis shows an average increase of 4.0% in the share of wind energy in these 14 states, compared to the normal days. In addition, most of the states where fossil power decreases during hot days belong to the Eastern Grid Interconnections, the biggest power grid in the United States, which allows them to better adjust power import during extreme events⁴¹. Furthermore, it's worth mentioning that the average population weighted Ta of 1795 extreme hot events in these 14 states is only 27.0 °C, which is only slightly higher than the widely used cooling Ta point, 26 °C, for U.S. states⁴². Less severe hot days making the cooling demand in the 14 states in the central region not so pronounced. This prompted us to set a critical Ta point (see Supplementary Methods) later in further analysis for comparing the impact of extreme cold days and hot days for the warm states and cold states (third section in Results).

The United States has three main electrical grids, or power interconnections, which are responsible for transmitting electricity within specific regions of the country⁴³: Eastern Interconnection, Western Interconnection and Texas Interconnection. We thus grouped the results into these three interconnections. There are 564 (11 states), 1833 (37 states), 59 (1 state), extreme cold days in Eastern, Western and Texas Interconnections, respectively. During extreme cold days, on average, the Texas Interconnection has the largest relative percent increase of 58.0% in terms of carbon emissions, compared to the normal Ta periods (Supplementary Methods). The Eastern and West Interconnections only show increasing emissions by 24.8% and 18.3%, during cold days relative to normal Ta periods. That is consistent with previous observations that larger power grids can provide greater stability and reliability for power systems^{44–46}. When climate extremes happen, the grid can draw on power from other regions or from a greater number of diverse sources, including renewable energy sources⁴⁷. This helps to mitigate the impact of weather-related disruptions on power systems. On the contrary, Texas's large emissions increase during cold days is partly due to its smallest and independent power grid⁴⁸. Further analysis indicates that the share of fossil fuels in the Texas Interconnections increased sharply by 18.5% (from 55.1% in normal winter days to 73.6% in extreme cold days) in extreme cold events, most of which is due to the large increase of share of natural gas by 18.4% from 34.8% in normal Ta period to 53.2% in extreme cold periods. On the other hand, the shares of oil and coal keeps relatively steady in extreme cold days. In addition,

frozen wind turbines given the high wind power installed capacity are another reason why Texas's carbon emissions were strongly affected by the winter storms^{49,50}. There's a clear reduction in the share of wind power from 31.3% to 15.1% (declined by 16.2%). The compound effect of increasing usage of natural gas and decreasing renewables finally leads to more carbon emissions generation and a higher carbon intensity during the 59 extreme cold days in Texas (Fig. 1). In this result, the extreme winter storm in February 2021^{6,48} lasted for 10 consecutive extreme cold days and accounted for 18.4% of the carbon emissions represented by all the 59 extreme cold days (Fig. 1, Fig. 2). For the East and West Interconnections, the average fossil energy share of all states within each grid are only increasing by 5.5% (from 54.2% to 59.7%) and 4.4% (from 51.3% to 55.7%) during cold days relative to normal winter days, respectively. Yet the share of coal, an energy source with a higher CO₂ emission factor, for these two interconnections was increasing by 3.0% and 1.8%, respectively. In general, the carbon intensity increased by 29.4% during extreme cold days for Texas interconnection, against 16.4% and 12.7% for the east and west interconnections. But, the average population-weighted Ta of cold extreme for the East and West Interconnections were much less severe than in Texas, with -8.1 °C (minimum Ta: -32.1 °C) and -4.9 °C (minimum Ta: -31 °C) compared to 3.1 °C (minimum Ta: -10 °C) in Texas. This result supports the hypothesis that larger power grids could mitigate the effect of climate extremes during cold extremes as well. Due to the limitation of available electricity transmission data within the grid, the mitigation impact caused by the electricity transmission deserves further investigation in the future study.

We detected 3427 (37 states), 1478 (11 states), 109 (1 state), extreme hot days in Eastern, Western and Texas Interconnections, respectively. In general, during extreme hot days, on average, the carbon emissions (and carbon intensity) for the three power grids were observed to increase by 13.6% (1.6%), 15.5% (8.3%), 2.3% (-6.1%) for east, west and Texas interconnections, respectively. For the Texas interconnection, the results show that the share of fossil fuel decreased by 4.6% during hot days (from 75.9% to 71.3%), because wind power increased by 5.7% (from 11.9–17.6%), which offset fossil fuels during the increased demand. Overall, our results indicate that wind energy is more negatively affected by extreme cold days than extreme hot days, because of frozen turbines in extreme cold conditions^{51,52}. Besides, extreme hot days seem to coincide with more potential wind resources and appropriate wind power conditions (obviously without risks of frozen temperature) (Supplementary Fig. 9).

Comparisons between extreme cold days and extreme hot days for warm states and cold states. In order to more accurately compare the two types of extreme events, we selected warmest states (with the top 12 highest annual mean temperatures,



see Supplementary Methods) and coldest states (with the top 12 lowest annual mean temperatures, see Supplementary Methods) in Fig. 3 (see Supplementary Methods and Supplementary Fig. 10). In addition, we further set a critical heating Ta point for extreme cold days ($15^{\circ}C$) and a cooling Ta point for extreme hot days ($26^{\circ}C$)⁴². This means that only cold events with extreme Ta and normal Ta less than $15^{\circ}C$ and hot events with extreme Ta and normal Ta larger than $26^{\circ}C$ are used in the comparisons

between both types of extreme events. This way, we can retain only the most extreme events, filtering out days without any actual heating or cooling demands.

During extreme cold days, carbon emissions increase by 4.2% as Ta declines by $1^{\circ}C$ in the warm states (Fig. 3). However, for cold states during extreme cold days, carbon emissions only increase by 1.5% as Ta declines by $1^{\circ}C$. This indicates that cold states have a smaller temperature sensitivity of their carbon

Fig. 3 Comparisons between cold states and warm states. **A** a and b represent the results for carbon emissions and intensity, respectively. Number 1, 2, 3 indicate extreme cold days in cold states, extreme cold days in warm states, and extreme hot days in warm states, respectively. The heating T_a point (15 °C in winter) and the cooling T_a point (26 °C in summer) were set as reference temperatures. For cold states in summer, even when the cooling T_a point is set as 24 °C, sufficient data points could not be collected, thus 26 °C was chosen as the threshold (see Supplementals). The X-axis represents the magnitude of temperature change: T_a decrease for panels 1 and 2 ($T_{a_{extreme}} < 5\%$ percentiles) and T_a increase for panels 3 ($T_{a_{extreme}} > 95\%$ percentiles). The red dashed line indicates the regression line. The label $avg(T_{a_{normal}})$ represents the average normal T_a for all the points in the plot, while $avg(T_{a_{extreme}})$ represents the average extreme T_a for all the points in the plot. N represents the number of points. P -value < 0.01 for all the results. **B** Uncertainty analysis using bootstrap for cold states and warm states. a and b indicate the results for Carbon Emission and Intensity change per unit temperature change. All the distributions indicate the 0 to 100 confidence intervals. Dashed line indicates the warm states. Solid line indicates the cold states. Blue color indicates the extreme cold days. Red color indicates the extreme hot days. The number of bootstrap simulations is 5000.

emissions, i.e., are more adapted to extreme cold days than warm states to cold days (Fig. 3 Panel A). Moreover, our uncertainty analysis indicates that the impact of extreme cold days in cold states are significantly lower than in warm states (Fig. 3 (Panel B) and Supplementary Fig. 12). The 95% confidence interval of the sensitivity of emissions to temperature of warm states in extreme cold days is [3.4, 5.0] %/°C, compared to that of cold states in extreme cold days with [1.2, 1.8]%/°C. The temperature sensitivity of carbon intensity in warm states is also larger than that in cold states during the extreme cold days. Carbon intensity increased by 2.2% as T_a declines by 1 °C for the warm states while in cold states, the carbon intensity only increased by 1.6% as T_a declines by 1 °C. We note, however, that the temperature sensitivity of carbon intensity for the warm states have higher confidence intervals of [1.5, 2.9] %/°C than cold states with [1.3, 1.9] %/°C during the extreme cold days. This implies that the variability in response to extreme cold days is larger among warm states than among cold states, which deserves to be further investigated.

For extremely hot days, even if considering only the days when the cooling threshold of 24 °C is exceeded, fewer data points are obviously retained for the cold states compared to the warm states (Supplementary Fig. 11). However, for warm states during extreme hot days, emissions are increasing by 3.5% when T_a increases by 1 °C. Compared to the temperature sensitivity of these warm states for extreme cold days, our results suggest that extreme cold days have more serious impacts on increasing emissions for a 1 °C cooling than extreme hot days for a 1 °C warming in warm states. But we also note that the two 95% confidence intervals show an overlap, which indicates a relatively large uncertainty in terms of the temperature sensitivity of carbon emission (Fig. 3, Supplementary Fig. 12). However, for the temperature sensitivity of the carbon intensity, extreme cold days shows significant more serious impact than extreme hot days with 95% confidence intervals of [1.5, 2.9] %/°C during extreme cold days, all with higher than the 95% confidence intervals of [0.5, 1.3] %/°C during extreme hot days in 5000 bootstrap simulations (Fig. 3, Supplementary Fig. 12). In general, the uncertainty analysis supports the hypothesis that (1) cold states are more adapted to extreme cold days than warm states. (2) Extreme cold days tend to have a higher temperature sensitivity of carbon emissions and intensity impact than extreme hot days for warm states.

We further analyze the duration of the two types of extreme events. Extreme hot events usually last longer than extreme cold events (Fig. 4) with an average duration of 6.2 ± 4.8 days for extreme hot days, compared to 4.1 ± 2.9 days for extreme cold days. The results show that during multi-days extreme cold events, carbon emissions show a significant increasing trend of 0.9% increase per day increase of event duration ($P < 0.01$) (relative to normal T_a periods) (Fig. 4). This trend is accompanied by a significant 1.2% increase per day increase of event duration for carbon intensity ($P < 0.01$) and 0.9% increase

per day increase of event duration for the fossil share in the total power production ($P < 0.01$) (Fig. 4a). Interestingly, we also find a significant reduction trend (1.2% reduction per day increase of event duration, $P < 0.01$) in the wind energy production as the extreme cold events duration increases (Supplementary Fig. 13). Part of this reason might be because of the frozen wind turbines. However, it's important to note that the increase in carbon emissions and carbon intensity is significantly influenced by concurrent drops in temperature compared to normal T_a periods. For instance, a continuous 7-day extreme cold event would result in a similar rise in emissions as three longer cold events lasting 11, 12, or 13 days. This similarity arises from the fact that these consecutive multi-day cold events exhibit comparable temperature declines when contrasted with normal T_a periods. This implies that temperature reductions, regardless of their duration, would lead to comparable increases in emissions during multi-day extreme cold events.

For extreme hot events, the increase of emissions also show a significant increasing trend of 0.7% increase per day increase of event duration ($P < 0.01$) relative to normal T_a periods, while carbon intensity and the share of fossil fuels doesn't show large variations as the event durations increase during the extreme hot events. This is partly because of the better renewable resources conditions such as strong solar generation, more potential wind resources and appropriate wind power conditions during extreme hot days, as discussed previously⁵³.

Comparisons between renewable dominated states and fossil energy dominated states. We categorized the 48 U.S. states plus D.C. into three power system categories: states dominated by renewable electricity generation (32 states), those dominated by fossil fuels electricity generation (7 states), and states dominated by nuclear electricity generation (3 states). The classification is based on having more than a 50% annual mean share of the specific energy sources in electricity production. The remaining states do not predominantly rely on a specific energy source for electricity generation.

Here, we further compare the renewables dominated states (defined as the states with more than 50% annual mean share of renewable energy in electricity production) and fossil dominated states (defined as the states with more than 50% annual mean share of fossil energy in the electricity production). Informed by our results in the last section about warm states and cold states, here we only keep the renewables dominated states and fossil energy dominated states with the same climate conditions (close annual mean air temperature) for further analysis. A bootstrap method was used to further check the impact of extreme cold/hot events for the two categories of states (Supplementary Methods). Figure 5 shows that for both extreme cold days or hot days, renewable dominated states all tend to have a higher mean carbon emissions/intensity increase per 1 °C. The emissions of renewable dominated states thus tend to be more affected by extreme temperature events, with higher mean carbon emissions increase

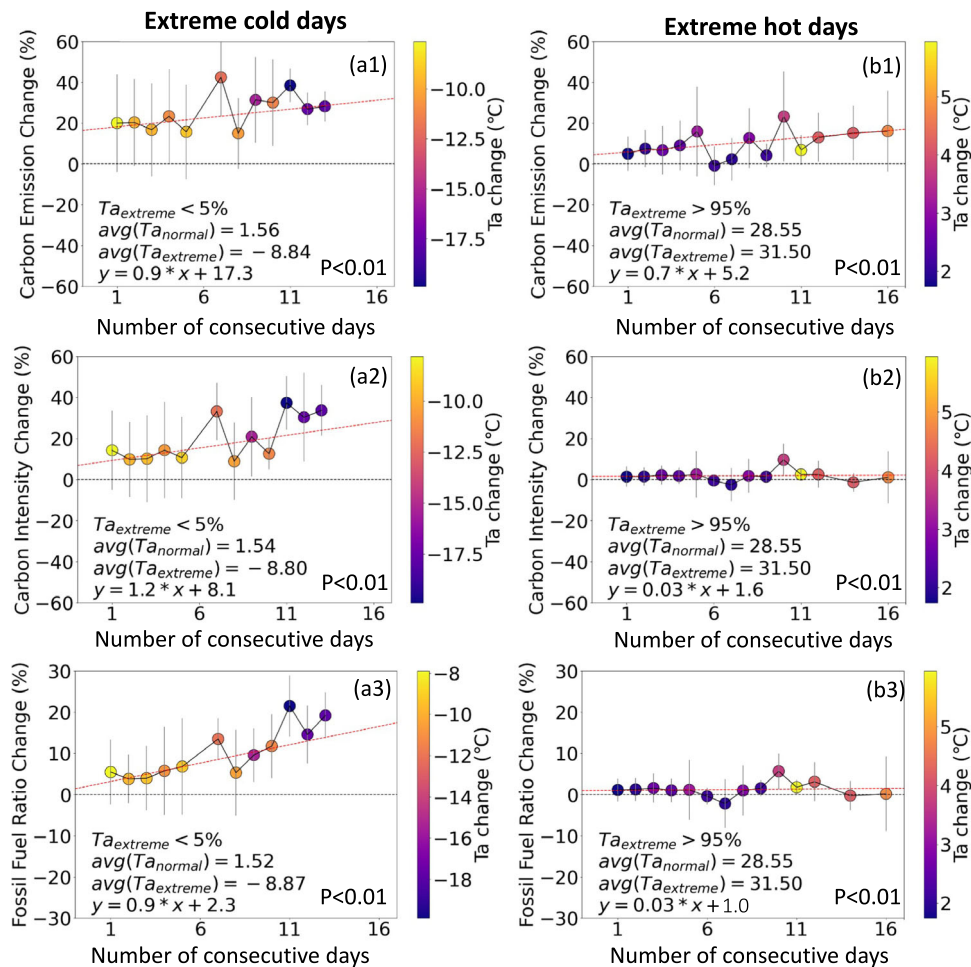


Fig. 4 The relationship between carbon emission and intensity changes and the number of consecutive days for extreme events. **a, b** For extreme cold days and extreme hot days, respectively. 1, 2, 3 for carbon emission, intensity and share of fossil fuel changes, respectively. X-axis indicates the number of consecutive days of the extreme events. The black dashed line indicates for the $y = 0$. Each dot represents the mean values of carbon emissions, carbon intensity and share of fossil fuels for the specific consecutive days' events. The gray lines indicate the standard deviations. Note that the colors of dots indicate the average air temperature differences between the extreme Ta days and the most recent normal Ta periods. The red dashed line indicates the regression line. P -value < 0.01 for a1, a2, a3, and b1, b2, b3. Note that we set the normal Ta less than $15\text{ }^{\circ}\text{C}$ in winter (heating Ta point), and the normal Ta larger than $26\text{ }^{\circ}\text{C}$ in summer (cooling Ta point).

per $1\text{ }^{\circ}\text{C}$ of $1.9\%/^{\circ}\text{C}$ during extreme cold days, and $2.8\%/^{\circ}\text{C}$ during extreme hot days, compared to $1.6\%/^{\circ}\text{C}$ and $1.7\%/^{\circ}\text{C}$ for fossil dominated states. In addition, renewables dominated states also show higher mean carbon intensity increase per $1\text{ }^{\circ}\text{C}$ of $2.2\%/^{\circ}\text{C}$ during extreme cold days, and $1.4\%/^{\circ}\text{C}$ during extreme hot days, compared to $1.5\%/^{\circ}\text{C}$ and $0.2\%/^{\circ}\text{C}$ for fossil energy dominated states. The significant difference is especially clearly seen in the impact of extreme hot days on carbon intensity. The uncertainty distributions could also imply other potential factors, which deserves to be further investigated.

Discussion

In summary, we first build a daily state-level power generation dataset for U.S. states and calculated the daily state-level carbon emission and carbon intensity. Based on this state-level dataset, we could quantify the impact of extreme events on the energy production and specifically impact of extreme cold events and hot events, on U.S. carbon emissions and carbon intensity. Finally, we further analyze the extreme events' intensity (defined by air temperature changes) and duration (consecutive days) of the two types of extreme events to provide a direct comparison between extreme hot days and cold days.

Our analysis mainly demonstrated that,

1. We found sharp increases of carbon intensity during extreme cold and hot days. As many studies reported increasing frequency and intensity of extreme events, our results suggest that more fossil emissions will be released in the future from extreme events.
2. In general, extreme temperature events increase carbon emissions and the reliance on fossil fuel power plants across the majority of the U.S. states. In addition, wind power reductions during extreme cold days and wind power increase during extreme hot days over the central U.S. are also clearly seen.
3. Cold states are more adapted to extreme cold days and increase their emissions less than warm states for a unit change of temperature. Therefore, our results suggest that extreme cold events have a more serious impact for increasing emissions than extreme hot events for warm states for a unit change of temperature. In addition, during extreme cold days, carbon emissions show a significant increasing trend per day increase of event duration. This trend is accompanied by a significant increasing trend of carbon intensity and fossil energy share per day increase of event duration.

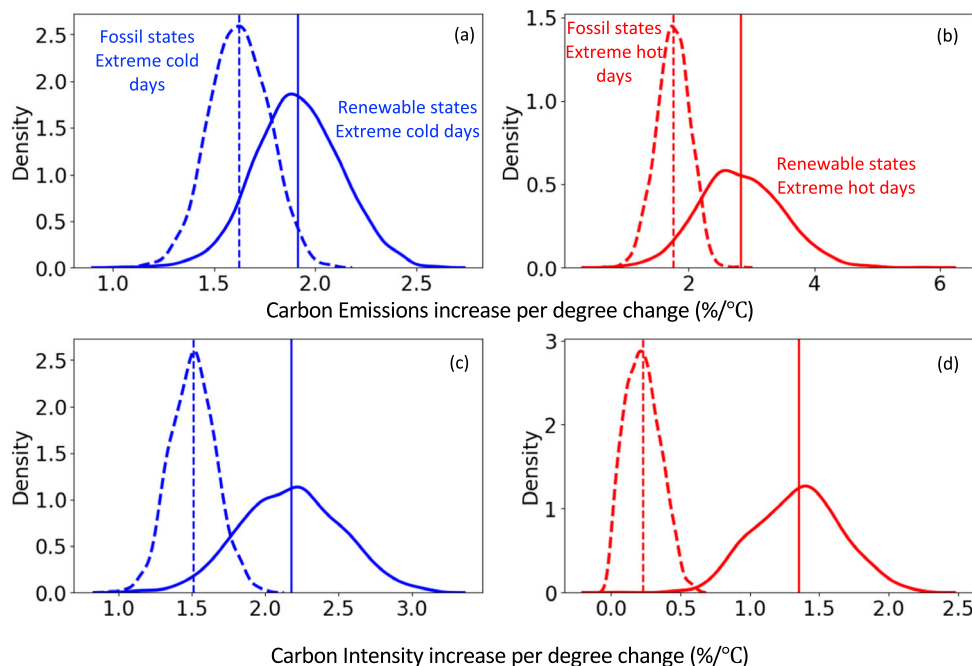


Fig. 5 Uncertainty analysis of the sensitivity of carbon emissions and carbon intensity to temperature for renewable dominated states and fossil energy dominated states. The upper and lower panels indicate the sensitivity of Carbon Emission and Intensity change per unit temperature change respectively. All the results indicate the whole 0 to 100 confidence intervals. Dashed line indicates the fossil dominated states. Solid line indicates the renewable dominated states. Blue color indicates the extreme cold days. Red color indicates the extreme hot days. The number of bootstrap simulations is 5000. Note that the fossil energy dominated states are the states with more than 50% annual mean share of fossil energy in electricity production. Correspondingly, the renewable dominated states are defined as the states with more than 50% annual mean share of renewable energy in electricity production.

- Carbon emissions and intensity in states with more renewable electricity generations tend to be more sensitive to extreme temperature events, with higher mean carbon emissions and intensity increase per 1 °C than in the states with more fossil electricity generations for both cold and hot days.

Overall, our study demonstrates for the first time, that extreme climate events can increase the carbon intensity of the energy production, increasing the reliance on carbonated sources of energy and reducing the capacity of renewables. To therefore achieve the goals of net zero emissions, the sizing and development of renewables should be made while accounting not only for changes in demand and mean climate but also countering impact of extreme events, which are increasing in frequency and intensity with climate change. This will pose a further challenge for the transition to a fully renewable-based electricity production system. Advances in large-scale energy storage techniques offer the potential for renewable energy systems to generate and store more electricity during favorable conditions, potentially mitigating the additional demand during extreme temperature events. However, it's important to note that further analysis and practical implementation are necessary to fully understand the response of power systems integrated with improved energy storage.

Data availability

The real-time hourly balancing authority-level electricity net generation dataset by energy source was downloaded from the U.S. Energy Information Administration (EIA) on-line database (<https://www.eia.gov/opendata/qb.php?category=3390101>). The population density data is from the GPWv4 dataset (<https://sedac.ciesin.columbia.edu/data/set/gpw-v4-population-density-rev11>). The air temperature data are from ERA5-Land reanalysis datasets (<https://cds.climate.copernicus.eu/cdsapp#!/dataset/reanalysis->

[era5-land?tab=overview](https://cds.climate.copernicus.eu/cdsapp#!/dataset/reanalysis-era5-land?tab=overview)). The processed dataset can be obtained from the following link: <https://doi.org/10.5281/zenodo.10161493>.

Code availability

The python code used to create the figures is available upon request from the corresponding author and will also be further accessed through Zenodo: <https://doi.org/10.5281/zenodo.10161493>.

Received: 9 March 2023; Accepted: 28 November 2023;
Published online: 13 December 2023

References

- IPCC. Climate change 2022: Impacts, adaptation and vulnerability. <https://hal.science/hal-03774939> (2022).
- Coumou, D. & Rahmstorf, S. A decade of weather extremes. *Nat. Clim. Change* **2**, 491–496 (2012).
- Fischer, E. M., Sippel, S. & Knutti, R. Increasing probability of record-shattering climate extremes. *Nat. Clim. Change* **11**, 689–695 (2021).
- Sun, Y. et al. Rapid increase in the risk of extreme summer heat in Eastern China. *Nat. Clim. Change* **4**, 1082–1085 (2014).
- Mueller, B., Zhang, X. & Zwiers, F. W. Historically hottest summers projected to be the norm for more than half of the world's population within 20 years. *Environ. Res. Lett.* **11**, 044011 (2016).
- Doss-Gollin, J., Farnham, D. J., Lall, U. & Modi, V. How unprecedented was the February 2021 Texas cold snap? *Environ. Res. Lett.* **16**, 064056 (2021).
- Shield, S. A., Quiring, S. M., Pino, J. V. & Buckstaff, K. Major impacts of weather events on the electrical power delivery system in the United States. *Energy* **218**, 119434 (2021).
- Larsen, P. H., Lawson, M., LaCommare, K. H. & Eto, J. H. Severe weather, utility spending, and the long-term reliability of the U.S. power system. *Energy* **198**, 117387 (2020).
- Larsen, P. H. et al. Projecting future costs to U.S. electric utility customers from power interruptions. *Energy* **147**, 1256–1277 (2018).

10. Panteli, M. & Mancarella, P. Influence of extreme weather and climate change on the resilience of power systems: Impacts and possible mitigation strategies. *Electr. Power Syst. Res.* **127**, 259–270 (2015).
11. Zuo, J. et al. Impacts of heat waves and corresponding measures: a review. *J. Clean. Prod.* **92**, 1–12 (2015).
12. Burillo, D., Chester, M. V., Ruddell, B. & Johnson, N. Electricity demand planning forecasts should consider climate non-stationarity to maintain reserve margins during heat waves. *Appl. Energy* **206**, 267–277 (2017).
13. Larcom, S., She, P.-W. & Van Gevelt, T. The UK summer heatwave of 2018 and public concern over energy security. *Nat. Clim. Change* **9**, 370–373 (2019).
14. Bazilian, M. et al. Considering the energy, water and food nexus: Towards an integrated modelling approach. *Energy Policy* **39**, 7896–7906 (2011).
15. Yalew, S. G. et al. Impacts of climate change on energy systems in global and regional scenarios. *Nat. Energy* **5**, 794–802 (2020).
16. Allen, M. R., Fernandez, S. J., Fu, J. S. & Olama, M. M. Impacts of climate change on sub-regional electricity demand and distribution in the southern United States. *Nat. Energy* **1**, 1–9 (2016).
17. Bartos, M. D. & Chester, M. V. Impacts of climate change on electric power supply in the Western United States. *Nat. Clim. Change* **5**, 748–752 (2015).
18. Paltán, H. A., Pant, R., Plummer Braeckman, J. & Dadson, S. J. Increased water risks to global hydropower in 1.5°C and 2.0°C Warmer Worlds. *J. Hydrol.* **599**, 126503 (2021).
19. Wan, W., Zhao, J., Popat, E., Herbert, C. & Döll, P. Analyzing the impact of streamflow drought on hydroelectricity production: a global-scale study. *Water Resour. Res.* **57**, (2021).
20. Ali, H. M. Recent advancements in PV cooling and efficiency enhancement integrating phase change materials based systems—A comprehensive review. *Sol. Energy* **197**, 163–198 (2020).
21. Wei, K., Yang, Y., Zuo, H. & Zhong, D. A review on ice detection technology and ice elimination technology for wind turbine. *Wind Energy* **23**, 433–457 (2020).
22. Schaeffer, R. et al. Energy sector vulnerability to climate change: A review. *Energy* **38**, 1–12 (2012).
23. The first big scare of the green era reveals grave problems with the transition to clean energy. *The Economist* https://www.economist.com/leaders/2021/10/16/the-first-big-energy-shock-of-the-green-era?utm_medium=affiliates.offer.pd&utm_source=partnerize-viglink&utm_campaign=a.io&utm_content=conversion.direct-response.anonymous&utm_term=1100lxXqYk6s&partnerize_clickref=1100lxXqYk6s (2021).
24. Höhne, N. et al. Wave of net zero emission targets opens window to meeting the Paris Agreement. *Nat. Clim. Change* **11**, 820–822 (2021).
25. Chen, L. et al. Strategies to achieve a carbon neutral society: a review. *Environ. Chem. Lett.* **20**, 2277–2310 (2022).
26. U.S. Energy Information Administration Website: <https://www.eia.gov/opendata/qb.php?category=3390101> (2023).
27. Muñoz-Sabater, J. et al. ERA5-Land: A state-of-the-art global reanalysis dataset for land applications. *Earth Syst. Sci. Data* **13**, 4349–4383 (2021).
28. Perera, A. T. D., Nik, V. M., Chen, D., Scartezzini, J.-L. & Hong, T. Quantifying the impacts of climate change and extreme climate events on energy systems. *Nat. Energy* **5**, 150–159 (2020).
29. Ombadi, M. & Risser, M. D. What's the temperature tomorrow? Increasing trends in extreme volatility of daily maximum temperature in Central and Eastern United States (1950–2019). *Weather Clim. Extrem.* **38**, 100515 (2022).
30. Jones, P. D., New, M., Parker, D. E., Martin, S. & Rigor, I. G. Surface air temperature and its changes over the past 150 years. *Rev. Geophys.* **37**, 173–199 (1999).
31. Ji, F., Wu, Z., Huang, J. & Chassignet, E. P. Evolution of land surface air temperature trend. *Nat. Clim. Change* **4**, 462–466 (2014).
32. Del Cueto, J. A. Comparison of energy production and performance from flat-plate photovoltaic module technologies deployed at fixed tilt. in *Conference Record of the Twenty-Ninth IEEE Photovoltaic Specialists Conference*, 2002. 1523–1526. <https://doi.org/10.1109/PVSC.2002.1190901> (IEEE, 2002).
33. Ali, H., Mahmood, M., Bashir, M., Ali, M. & Siddiqui, A. Outdoor testing of photovoltaic modules during summer in Taxila, Pakistan. *Therm. Sci.* **20**, 165–173 (2016).
34. Amin, N., Lung, C. W. & Sopian, K. A practical field study of various solar cells on their performance in Malaysia. *Renew. Energy* **34**, 1939–1946 (2009).
35. Meneses-Rodríguez, D., Horley, P. P., González-Hernández, J., Vorobiev, Y. V. & Gorley, P. N. Photovoltaic solar cells performance at elevated temperatures. *Sol. Energy* **78**, 243–250 (2005).
36. Delucchi, M. A. & Jacobson, M. Z. Providing all global energy with wind, water, and solar power, Part II: Reliability, system and transmission costs, and policies. *Energy Policy* **39**, 1170–1190 (2011).
37. Sun, W. & Harrison, G. P. Wind-solar complementarity and effective use of distribution network capacity. *Appl. Energy* **247**, 89–101 (2019).
38. Chen, L. Impacts of climate change on wind resources over North America based on NA-CORDEX. *Renew. Energy* **153**, 1428–1438 (2020).
39. U.S. Energy Information Administration Website <https://www.eia.gov/todayinenergy/detail.php?id=46976> (2021).
40. U.S. Energy Information Administration Website <https://www.eia.gov/energyexplained/wind/where-wind-power-is-harnessed.php> (2023).
41. Liu, Z. *Global energy interconnection*. (Academic Press, 2015).
42. Wang, H. & Chen, Q. Impact of climate change heating and cooling energy use in buildings in the United States. *Energy Build* **82**, 428–436 (2014).
43. U.S. department of energy website <https://www.energy.gov/oe/learn-more-about-interconnections> (2023).
44. Hoke, A. et al. Island power systems with high levels of inverter-based resources: Stability and reliability challenges. *IEEE Electrification Mag* **9**, 74–91 (2021).
45. Kundur, P. S. & Malik, O. P. *Power system stability and control*. (McGraw-Hill Education, 2022).
46. Rogers, G. The nature of power system oscillations. in *Power System Oscillations 7–30* (Springer, 2000).
47. Jufri, F. H., Widiputra, V. & Jung, J. State-of-the-art review on power grid resilience to extreme weather events: definitions, frameworks, quantitative assessment methodologies, and enhancement strategies. *Appl. Energy* **239**, 1049–1065 (2019).
48. Busby, J. W. et al. Cascading risks: understanding the 2021 winter blackout in Texas. *Energy Res. Soc. Sci.* **77**, 102106 (2021).
49. Gruber, K., Gauster, T., Laaha, G., Regner, P. & Schmidt, J. Profitability and investment risk of Texan power system winterization. *Nat. Energy* **7**, 409–416 (2022).
50. Gao, L. & Hu, H. Wind turbine icing characteristics and icing-induced power losses to utility-scale wind turbines. *Proc. Natl. Acad. Sci.* **118**, e2111461118 (2021).
51. Etemaddar, M., Hansen, M. O. L. & Moan, T. Wind turbine aerodynamic response under atmospheric icing conditions. *Wind Energy* **17**, 241–265 (2014).
52. Hu, L., Zhu, X., Hu, C., Chen, J. & Du, Z. Wind turbines ice distribution and load response under icing conditions. *Renew. Energy* **113**, 608–619 (2017).
53. Tong, D. et al. Geophysical constraints on the reliability of solar and wind power worldwide. *Nat. Commun.* **12**, 6146 (2021).

Acknowledgements

P.G. would like to acknowledge funding from European Research Council grant USMILE and National Science Foundation Science and Technology Center LEAP, Learning the Earth with Artificial intelligence and Physics, as well as support from NASA grant 80NSSC18K0998. W. Z. would like to acknowledge the support from the Carbon Monitor project (<https://carbonmonitor.org/>) and the scholarship awarded by the Max Planck Institute for Biogeochemistry. The authors also thank Julianne DeAngelo for help analyzing AR6 scenarios.

Author contributions

W.Z., P.G., S.J.D., P.C. and Z.L. designed the study. W.Z. performed the analyses, with additional support from B.Z. and H.C. on datasets and analytical approaches. W.Z., P.G., S.J.D. and P.C. led the writing with input from all coauthors.

Competing interests

The authors declare no competing interests.

Additional information

Supplementary information The online version contains supplementary material available at <https://doi.org/10.1038/s43247-023-01147-z>.

Correspondence and requests for materials should be addressed to Wenli Zhao or Pierre Gentine.

Peer review information *Communications Earth & Environment* thanks the anonymous reviewers for their contribution to the peer review of this work. Primary Handling Editors: Prabir Patra and Aliénor Lavergne. A peer review file is available.

Reprints and permission information is available at <http://www.nature.com/reprints>

Publisher's note Springer Nature remains neutral with regard to jurisdictional claims in published maps and institutional affiliations.



Open Access This article is licensed under a Creative Commons Attribution 4.0 International License, which permits use, sharing, adaptation, distribution and reproduction in any medium or format, as long as you give appropriate credit to the original author(s) and the source, provide a link to the Creative Commons license, and indicate if changes were made. The images or other third party material in this article are included in the article's Creative Commons license, unless indicated otherwise in a credit line to the material. If material is not included in the article's Creative Commons license and your intended use is not permitted by statutory regulation or exceeds the permitted use, you will need to obtain permission directly from the copyright holder. To view a copy of this license, visit <http://creativecommons.org/licenses/by/4.0/>.

© The Author(s) 2023